Modeled and observed properties related to the direct aerosol radiative effect of biomass burning aerosol over the Southeast Atlantic

Sarah J. Doherty[1,2], Pablo E. Saide[3,4], Paquita Zuidema[5], Yohei Shinozuka[6,7], Gonzalo A. Ferrada[8], Hamish Gordon[9], Marc Mallet[10], Kerry Meyer[11], David Painemal[12,13], Steven G. Howell[14], Steffen Freitag[14], Amie Dobracki[5], James R. Podolske[7], Sharon P. Burton[13], Richard A. Ferrare[13], Calvin Howes[3], Pierre Nabat[10], Gregory R. Carmichael[8], Arlindo da Silva[15], Kristina Pistone[6,7], Ian Chang[16], Lan Gao[16], Robert Wood[2] and Jens Redemann[16]

[1] Cooperative Institute for Climate, Ocean and Ecosystem Studies, Seattle, WA, USA
[2] Department of Atmospheric Science, University of Washington, Seattle, WA, USA
[3] Department of Atmospheric and Oceanic Sciences, University of California, Los Angeles, CA USA
[4] Institute of the Environment and Sustainability, University of California, Los Angeles, CA, USA
[5] Rosenstiel School of Marine and Atmospheric Science, University of Miami, Miami, FL, USA
[6] Bay Area Environmental Research Institute, Moffett Field, CA, USA
[7] NASA Ames Research Center, Moffett Field, CA, USA
[8] Center for Global and Regional Environmental Research, The University of Iowa, Iowa City, IA, USA
[9] Engineering Research Accelerator and Center for Atmospheric Particle Studies, Carnegie Mellon University, Pittsburgh, PA, USA
[10] CNRM, Université de Toulouse, Météo-France, CNRS, Toulouse, France
[11] NASA Goddard Space Flight Center, Greenbelt, Maryland, MD 20771, USA
[12] Science Systems and Applications Inc., Hampton, Virginia 23666, USA
[13] NASA Langley Research Center, Hampton, Virginia 23691 USA
[14] University of Hawaii at Manoa, Honolulu, HI, USA
[15] Global Modeling and Assimilation Office, NASA Goddard Space Flight Center, Greenbelt, MD, USA
[16] School of Meteorology, University of Oklahoma, Norman, OK, USA

Correspondence to: Sarah J. Doherty (sarahd@atmos.washington.edu)

SUPPLEMENTAL INFORMATION

Table S1. Coordinates of the four transects of gridboxes used in this comparison. Gridboxes are numbered 1-8 (Diagonal, Meridional) or 1-11 (Zonal) from west to east and/or north to south.

Transect Name	Year(s)	Latitude	Longitude
Diagonal†	2016	7-11S 9-13S 11-15S 13-17S 15-19S 17-21S 19-23S 21-25S	2W-2E 0-4E 2-6E 4-8E 6-10E 8-12E 10-14E 12-16E
Meridional1	2016	7-9S 9-11S 11-13S 13-15S 15-17S 17-19S 19-21S 21-23S	9-11.75E
Zonal	2016, 2017	6-10S	15-13W 13-11W 11-9W 9-7W 7-5W 5-3W 3-1W 1W-1E 1-3E 3-5E 5-7E
Meridional2	2017, 2018	0.5N-1.5S 1.5-3.5S 3.5-5.5S 5.5-7.5S 7.5-9.5S 9.5-11.5S 11.5-13.5S 13.5-15.5S	4-6E

†For the Diagonal transect, coordinates given are for the latitudes of the north and south corners and the longitudes of the east and west corners of the gridbox.

Table S.2: The difference between the average of CF_{warm} at 10:30 and 13:30 and CF_{warm} for all times when SZA<75° (i.e. the expected ratio of MODIS daily avg CF_{warm} vs SEVIRI daily avg CF_{warm}) during the three field campaign periods

a) Zonal Transect			
Gridbox (W->E)	**2016**	**2017**	**2018**
1	-0.025	-0.009	-0.010
2	-0.030	0.002	-0.010
3	-0.034	0.007	-0.006
4	-0.024	-0.021	-0.008
5	-0.013	-0.027	-0.008
6	-0.023	-0.016	-0.003
7	-0.024	-0.018	0.004
8	-0.023	-0.018	0.001
9	-0.030	-0.013	-0.015
10	-0.038	-0.020	-0.014
11	-0.042	-0.032	-0.001
mean	*-0.053*	*-0.081*	*0.000*
std dev	*-0.063*	*-0.081*	*0.009*

b) Diagonal Transect	
Gridbox (NW->SE)	**2016**
1	-0.007
2	-0.004
3	-0.007
4	-0.030
5	-0.024
6	0.002
7	-0.007
8	-0.010
mean	*-0.011*
std dev	*0.011*

c) Meridional1 Transect	
Gridbox (N->S)	**2016**
1	-0.094
2	-0.143
3	-0.135
4	-0.090
5	-0.030
6	0.053
7	0.051
8	0.094
mean	*-0.037*
std dev	*0.092*

d) Meridional2 Transect		
Gridbox (N->S)	**2017**	**2018**
1	-0.080	0.105
2	-0.068	0.102
3	-0.040	0.040
4	-0.058	-0.053
5	-0.008	-0.079
6	0.012	-0.096
7	-0.012	-0.081
8	-0.034	-0.115
mean	*-0.036*	*-0.022*
std dev	*0.032*	*0.090*

Table S.3: As in Table S.2, but showing the difference in median COT_{warm} at 10:30 and 13:30 versus the median for the full daytime, based on an empirical fit to COT_{warm} versus CF_{warm} from the MODIS-ACAERO retrievals.

a) Zonal Transect			
Gridbox (W->E)	**2016**	**2017**	**2018**
1	-0.37	-0.16	-0.27
2	-0.41	-0.06	-0.66
3	-0.50	0.00	-0.85
4	-0.38	-0.30	-0.73
5	-0.23	-0.42	-0.85
6	-0.39	-0.27	-0.58
7	-0.41	-0.29	-0.46
8	-0.41	-0.30	-0.37
9	-0.51	-0.24	-0.54
10	-0.63	-0.36	-0.34
11	-0.66	-0.51	-0.34
mean	*-0.78*	*-1.05*	*-0.06*
std dev	*-0.88*	*-0.97*	*-0.38*

b) Diagonal Transect	
Gridbox (NW->SE)	**2016**
1	-0.14
2	-0.08
3	-0.14
4	-0.50
5	-0.37
6	0.01
7	-0.12
8	-0.11
mean	*-0.18*
std dev	*0.17*

c) Meridional1 Transect	
Gridbox (N->S)	**2016**
1	-1.03
2	-1.12
3	-0.79
4	-0.58
5	-0.43
6	-0.38
7	-0.01
8	0.22
mean	*-0.52*
std dev	*0.47*

d) Meridional2 Transect		
Gridbox (N->S)	**2017**	**2018**
1	-0.96	-0.02
2	-0.82	-0.06
3	-0.49	-0.21
4	-0.67	-0.39
5	-0.20	-0.45
6	0.19	-0.29
7	-0.23	-0.51
8	-0.61	-0.32
mean	*-0.48*	*-0.28*
std dev	*0.38*	*0.18*

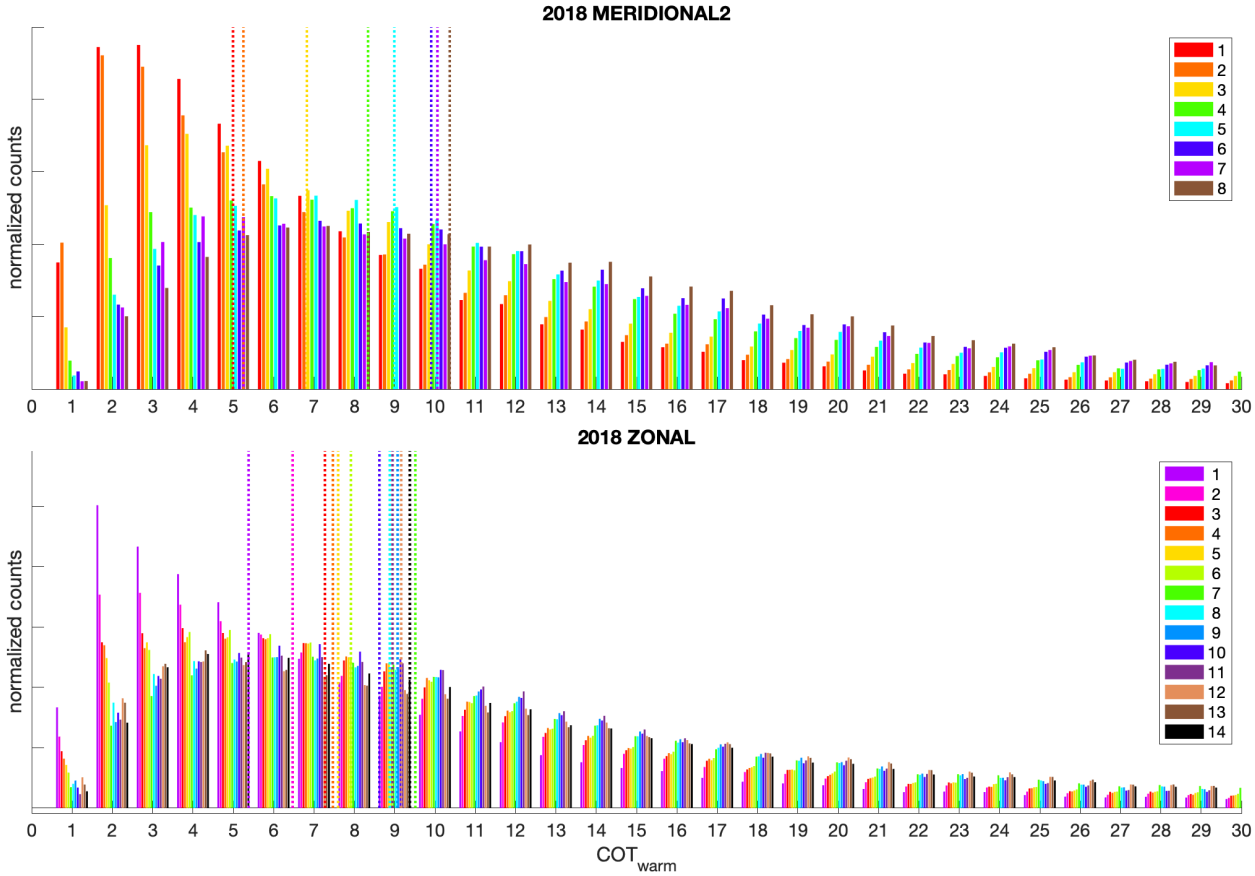

Figure S.1 A histogram of COT_{warm} from the MODIS-ACAERO retrievals for the 2018 Meridional2 and Zonal transects, colored by transect gridbox number (Figure 1). COT_{warm} for the transects in 2016 and 2018 have similarly shaped distributions.

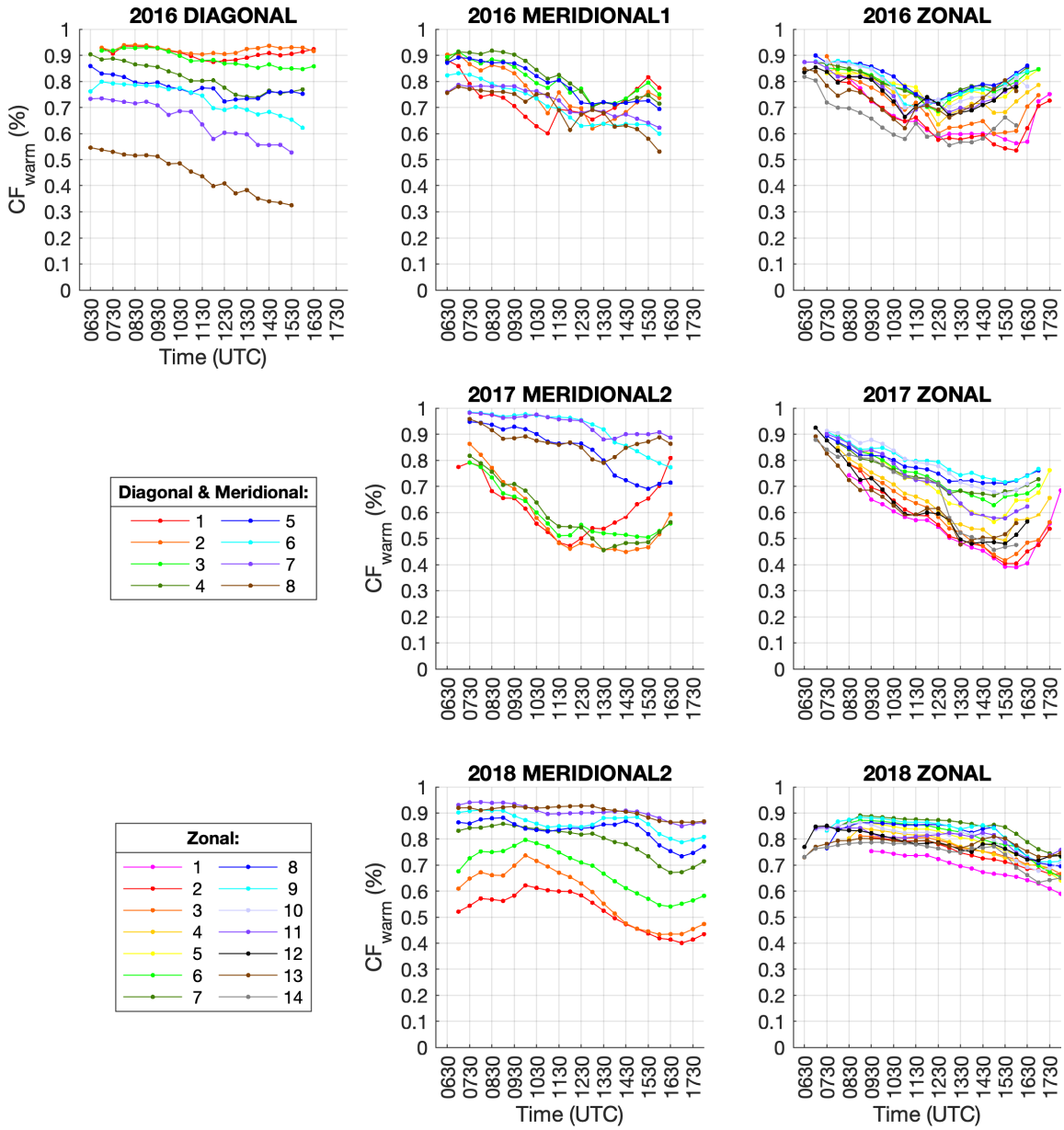

Figure S.2 CF_{warm} from the SEVIRI-LaRC retrievals, for all times when SZA<75°, showing the diurnal cycle in CF across the comparison gridboxes during the dates of the ORACLES field campaigns in 2016, 2017 and 2018.

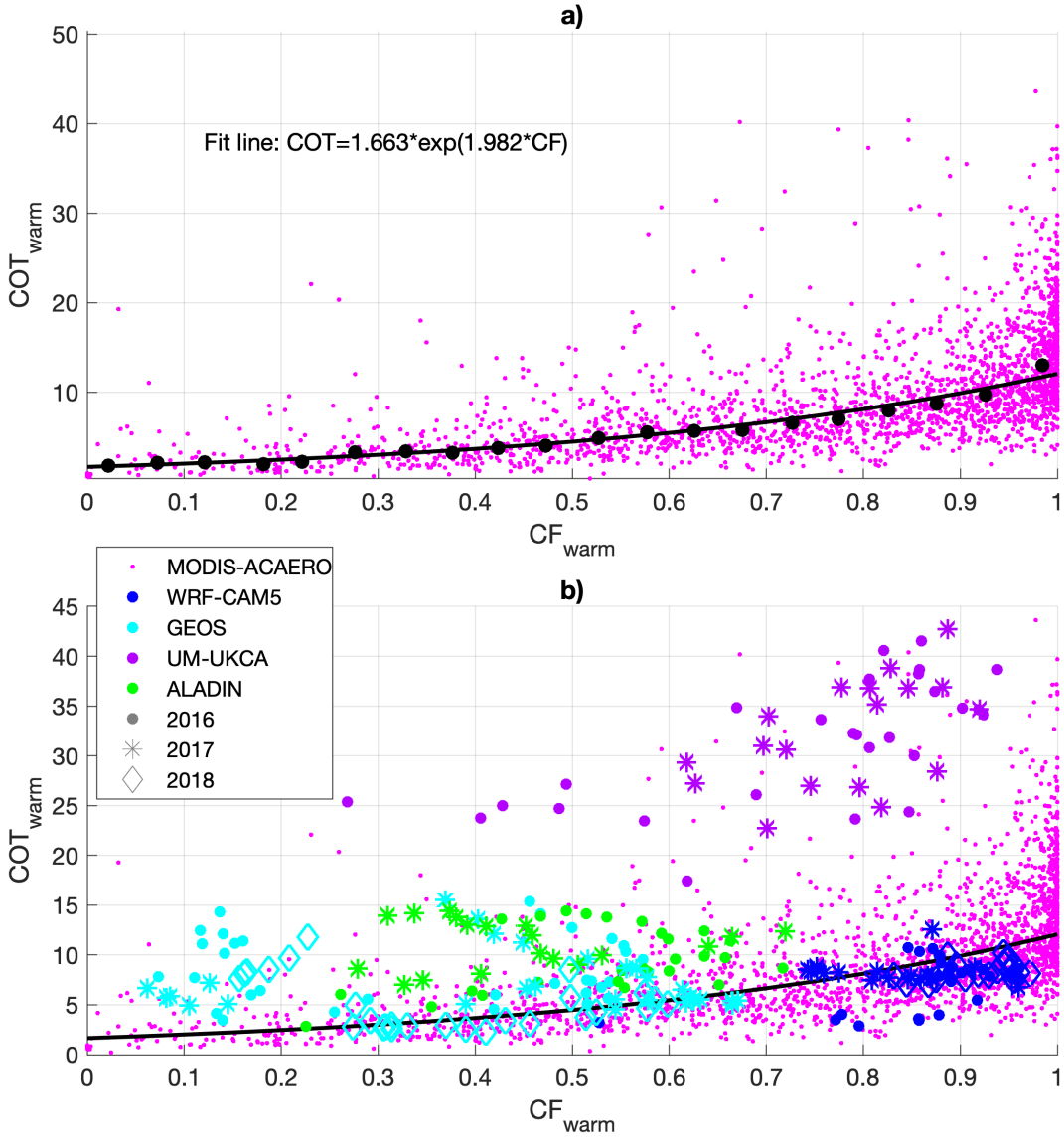

Figure S.3 COT_{warm} versus CF_{warm} for a) pixel-level MODIS-ACAERO retrievals, with an empirical fit using averages (blue dots) in CF_{warm} bins of 0.05, and b) for both MODIS-ACAERO pixel-level retrievals gridbox averages from the four models included in this comparison.

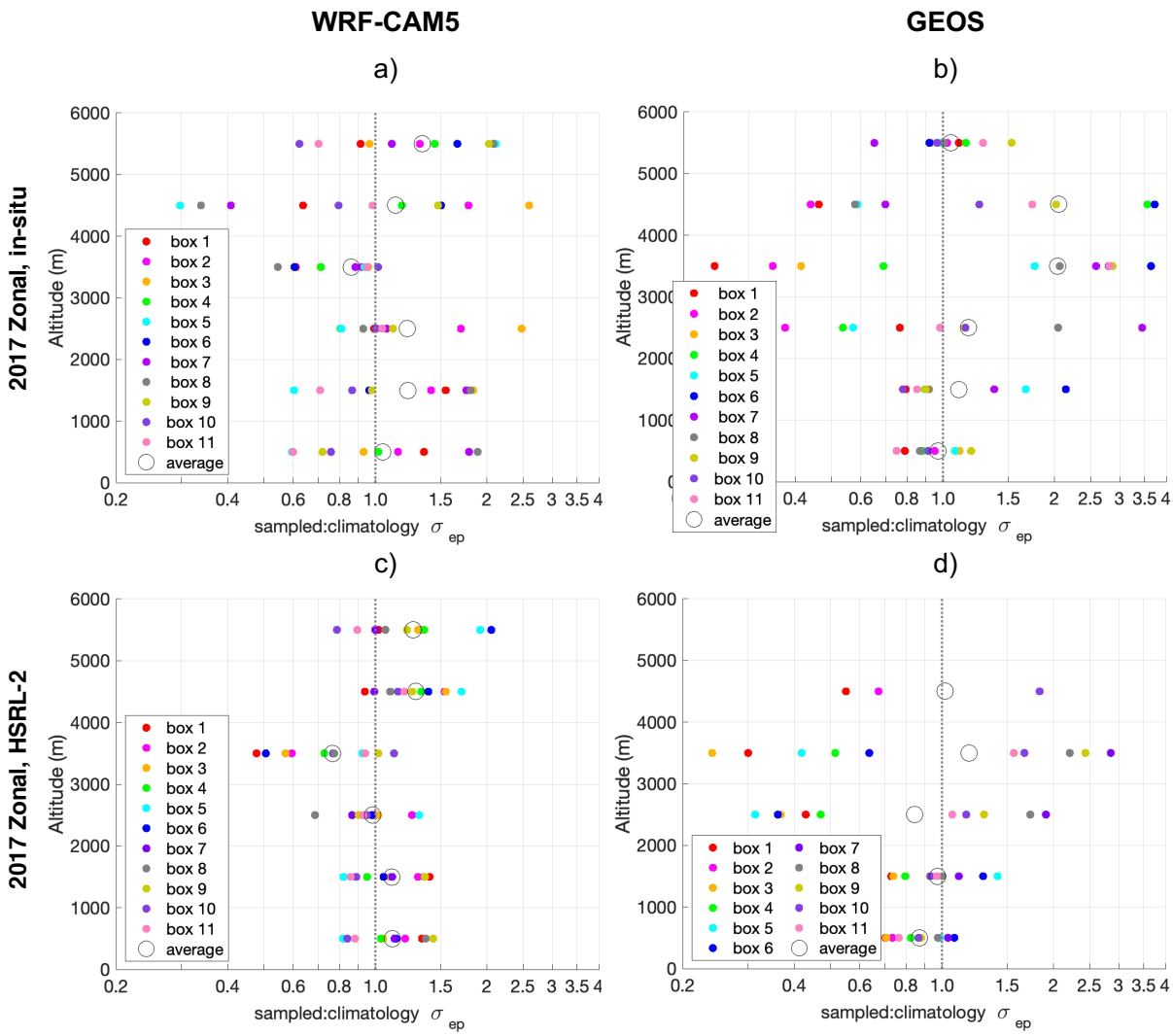

Figure S.4 As in Figure 3: Plots showing the representativeness of the in -situ (a and b) and HSRL-2 (c and d) sampled values of σ_{ep} for the 2017 Zonal transect from WRF-CAM5 simulations (a and c) and GEOS simulations (b and d).

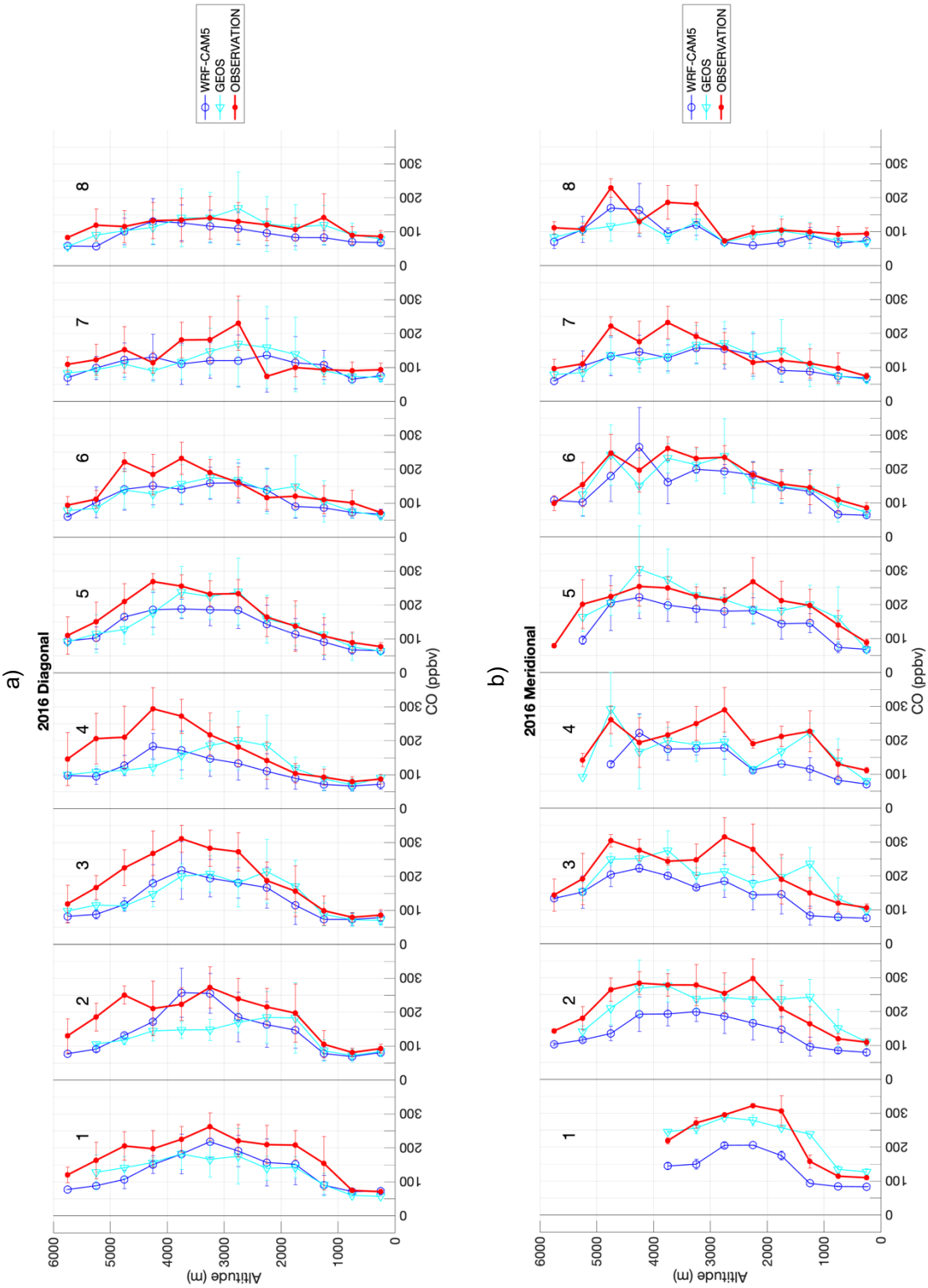
a)
2016 Diagonal
WRF-CAM5
GEOS
OBSERVATION
Altitude (m)
CO (ppbv)
b)
2016 Meridional
WRF-CAM5
GEOS
OBSERVATION
Altitude (m)
CO (ppbv)

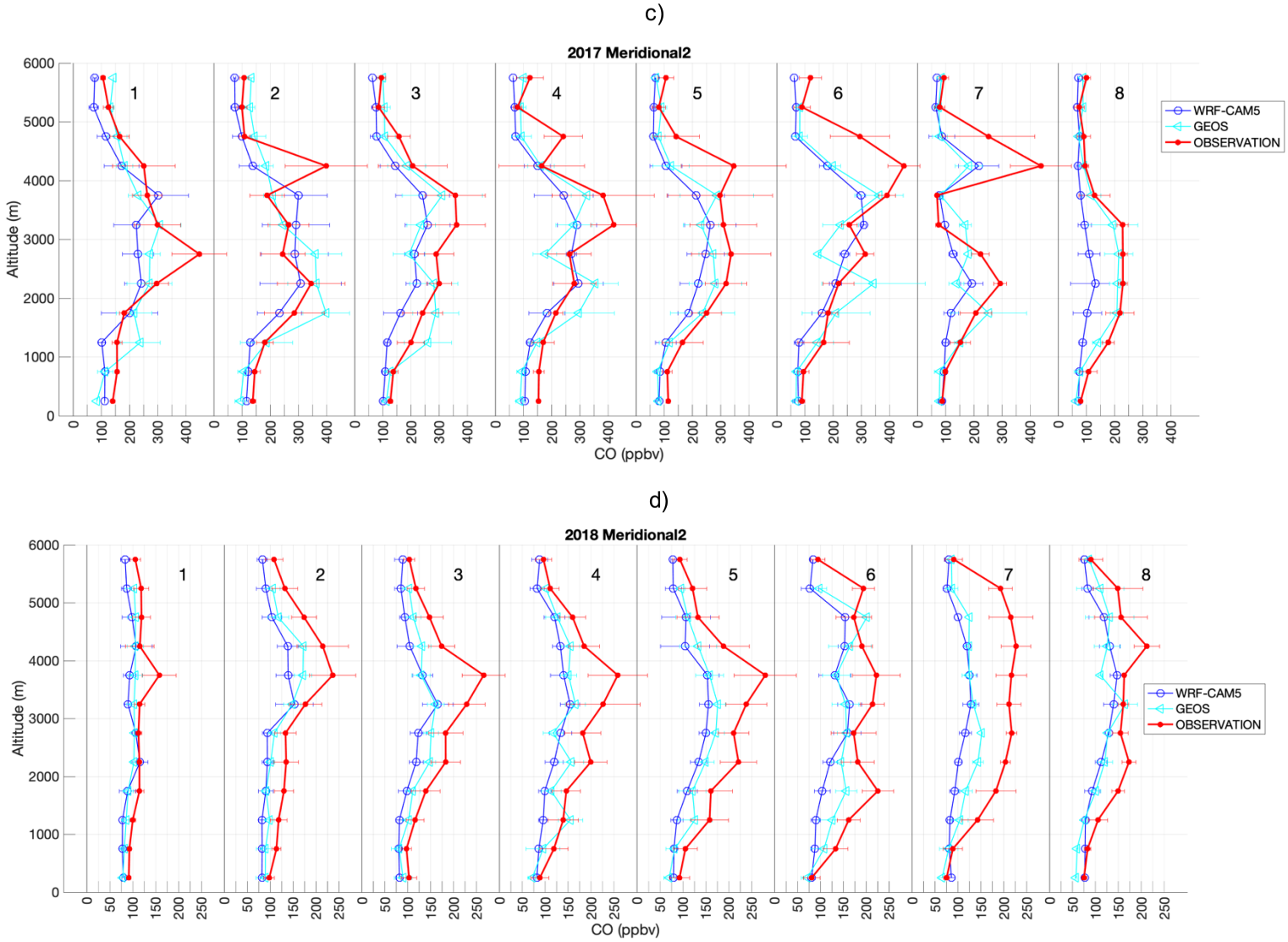

Figure S.5 As in Figure 4, but for profiles of carbon monoxide (CO) mixing ratio.

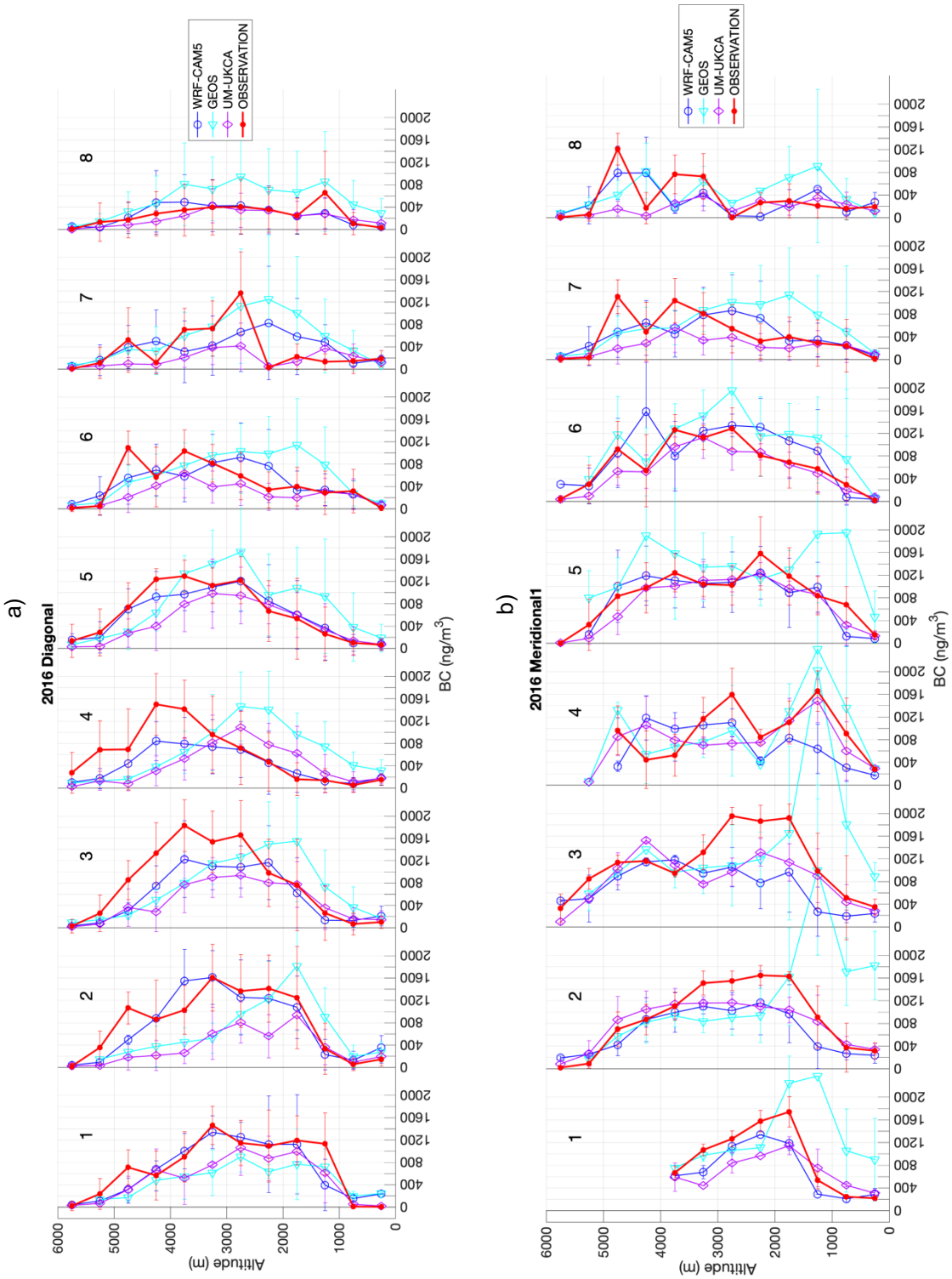
a)
2016 Diagonal
b)
2016 Meridional1
WRF-CAM5
GEOS
UM-UKCA
OBSERVATION
Altitude (m)
BC (ng/m3)
1
2
3
4
5
6
7
8

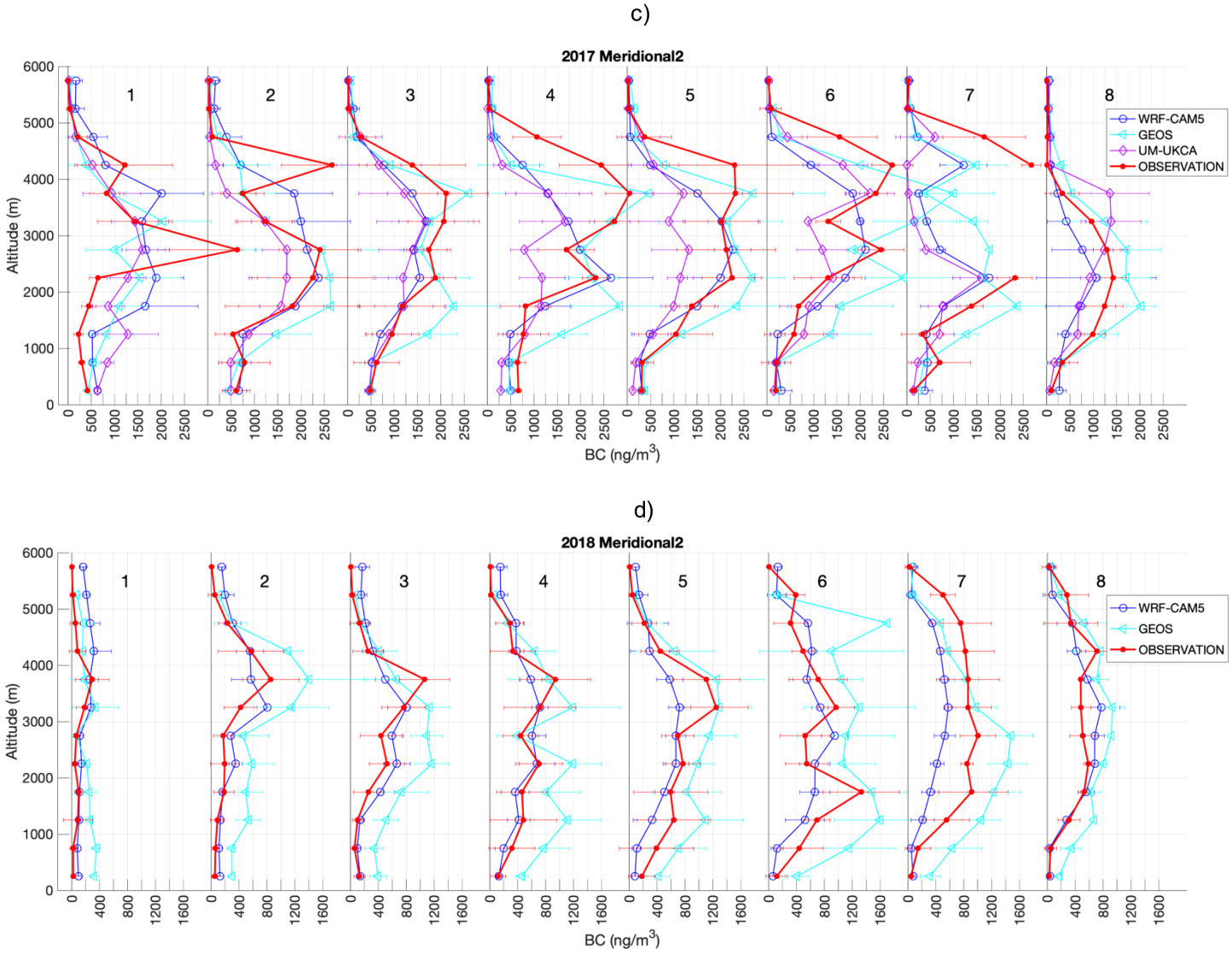

Figure S.6 As in Figure 4, but for black carbon (BC) mass concentration.

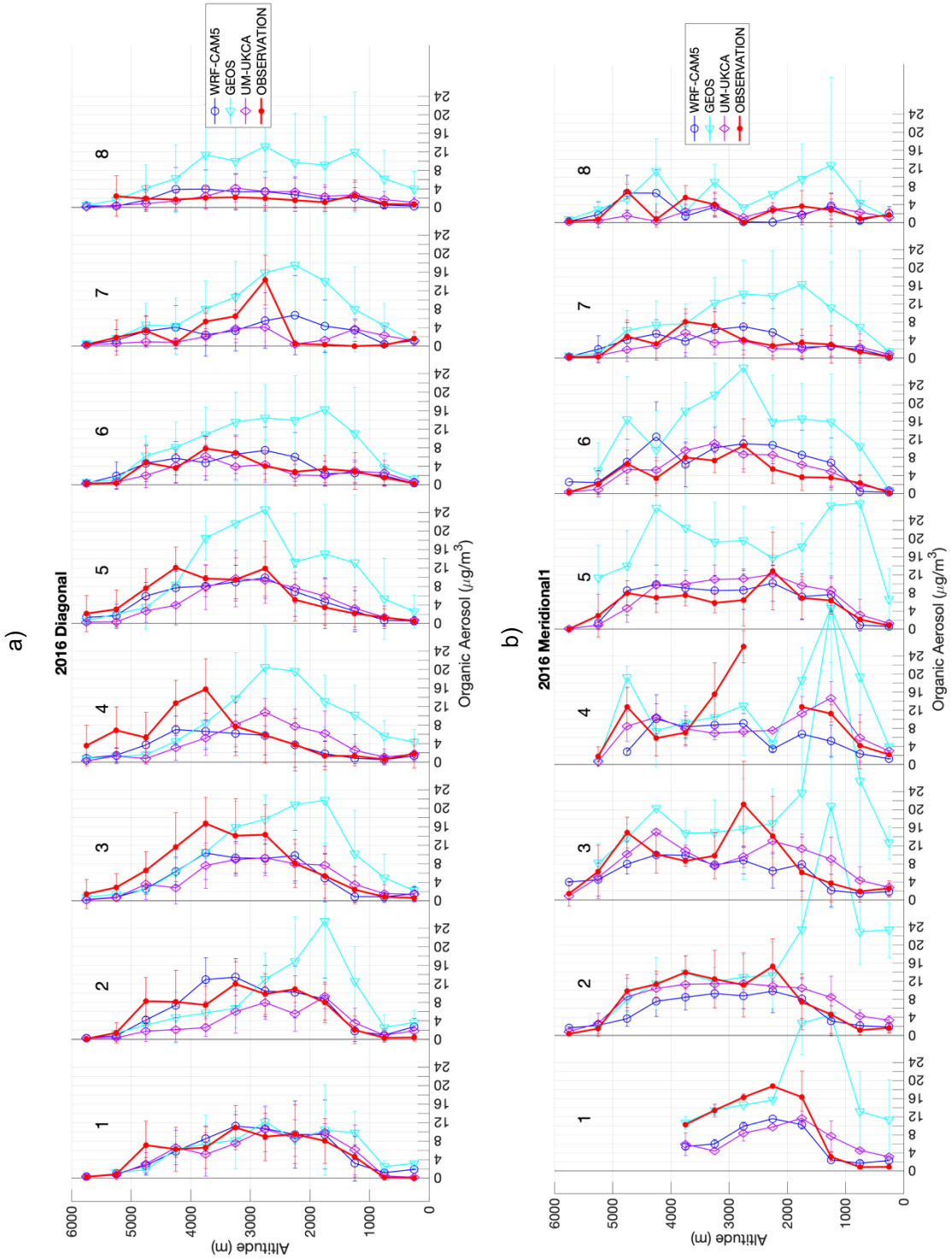
a)
2016 Diagonal
WRF-CAM5
GEOS
UM-UKCA
OBSERVATION
Altitude (m)
Organic Aerosol (μg/m3)
b)
2016 Meridional1
WRF-CAM5
GEOS
UM-UKCA
OBSERVATION
Altitude (m)
Organic Aerosol (μg/m3)

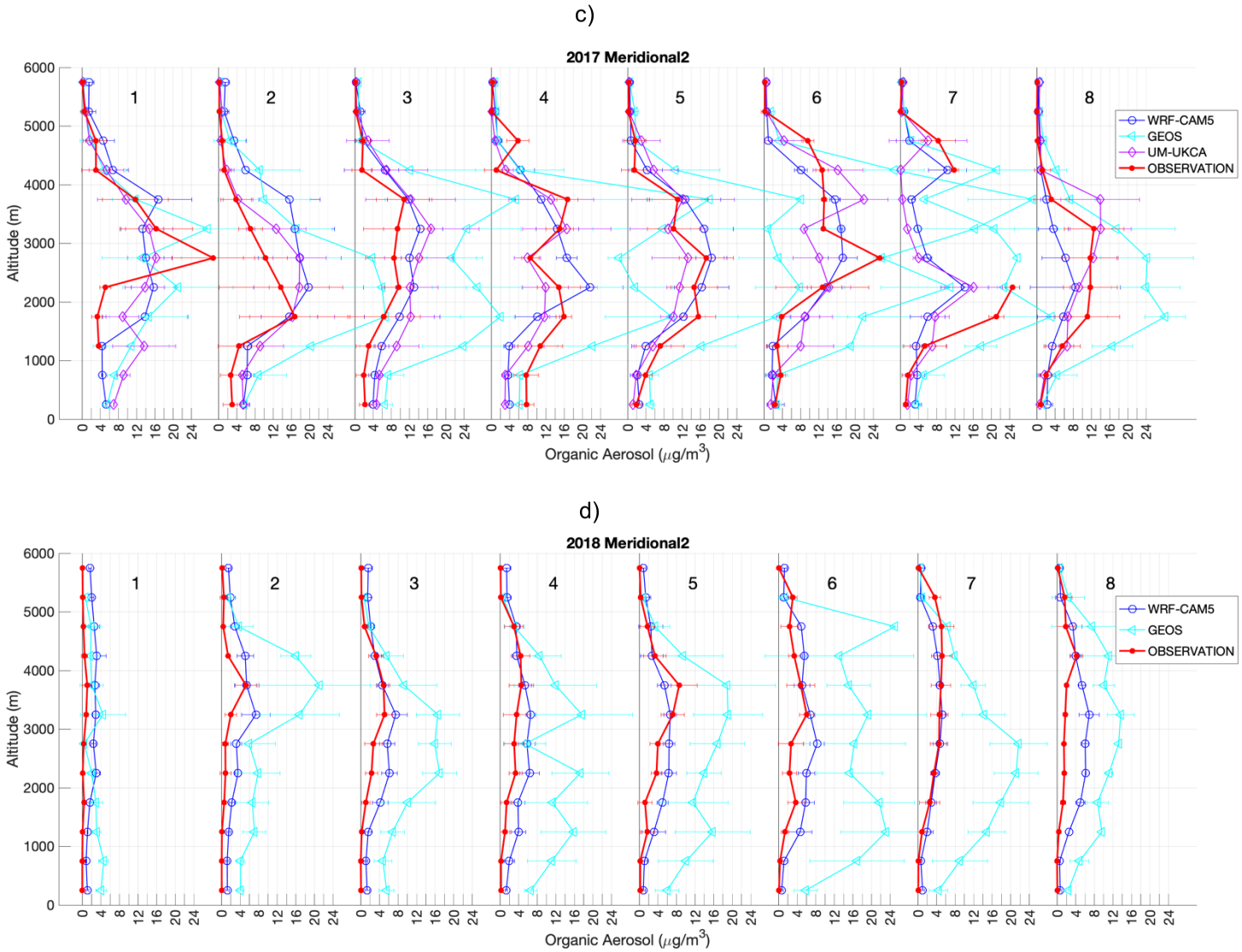

Figure S.7 As in Figure 4, but for organic aerosol (OA) mass concentration.

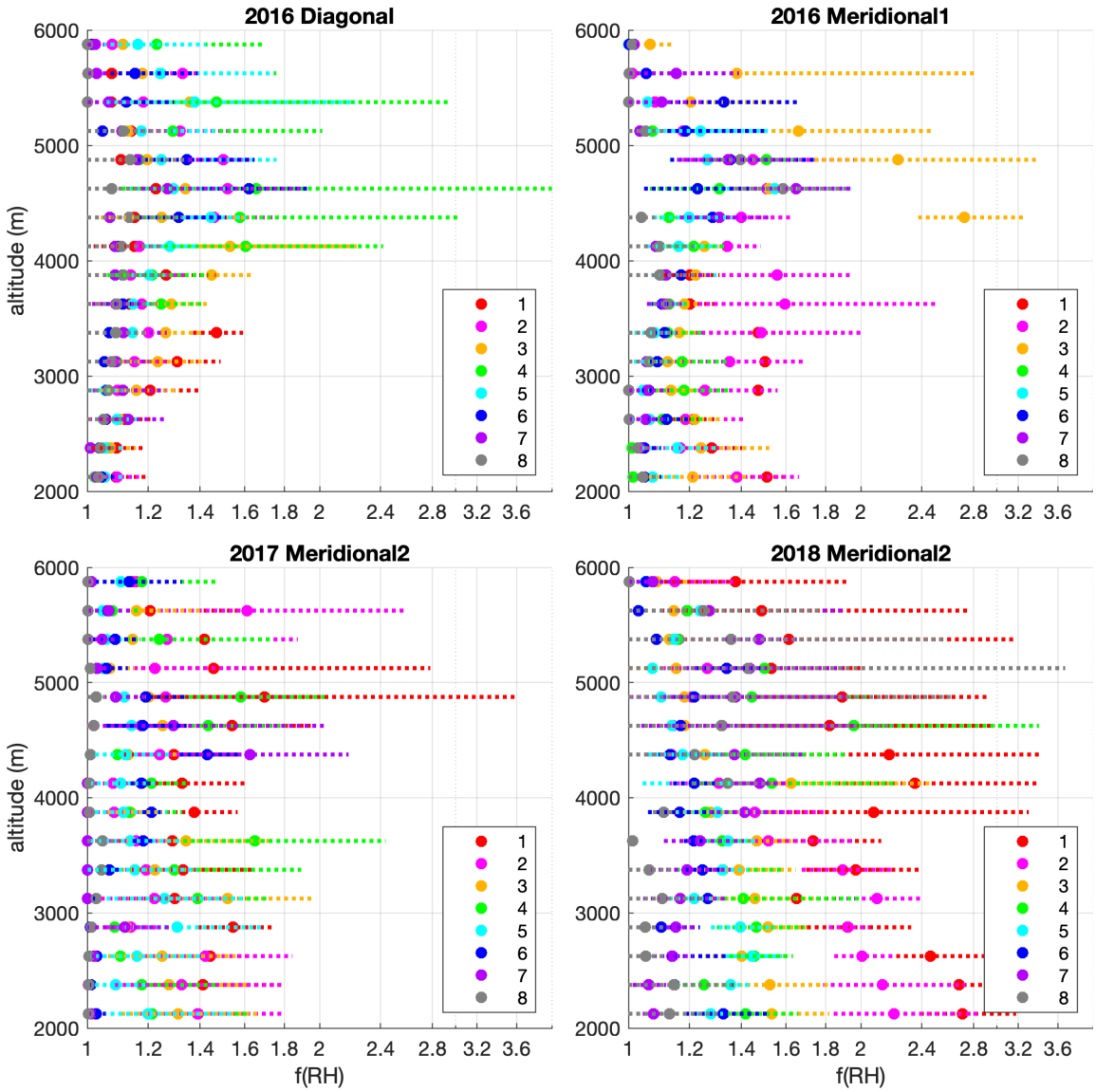

Figure S.8 Light scattering (σ_{sp}) humidification factor, f(RH), estimated for adjusting from the measured in-situ at low RH to ambient RH. This estimate uses the gamma fit to low and high (approx. 80%) RH light scattering measured in-situ in the P-3 aircraft, averaged for all data 2-5km altitude where σ_{sp}>25 Mm^{-1}. The campaign-wide averages from 2016 (γ=0.62) and 2018 (γ=0.62; used for both 2017 and 2018) are used with observed ambient RH (Figure 6) to calculate the f(RH) values shown here. Solid dots are f(RH) for the gridbox-mean ambient RH and the dashed horizontal bars for +/-1 sigma in ambient RH, with f(RH) truncated at 1.0 in the lower limit. Colors indicate the gridbox number, as shown in Figure 1.

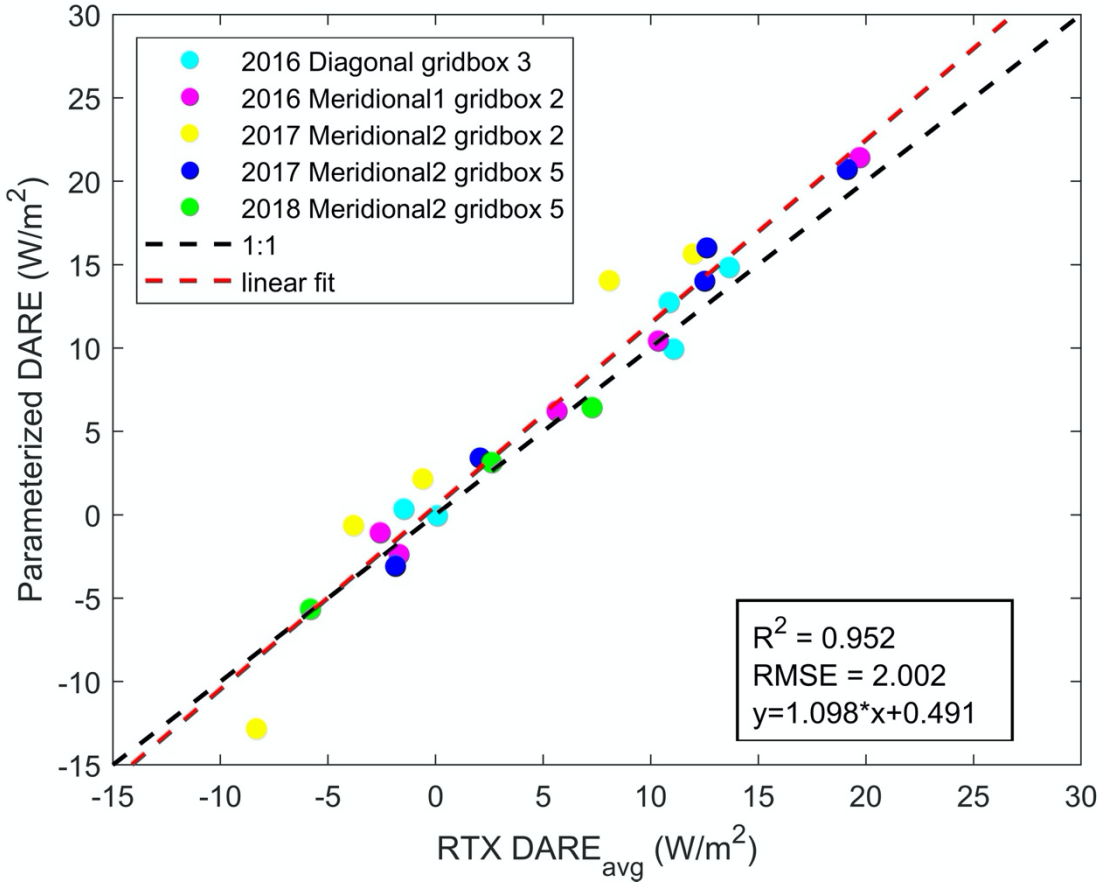

Figure S.9 Comparison of parameterized DARE from Equation [3] versus DARE from full radiative transfer calculations, as described in the text.